Molecular Biology of the Cell
Vol. 9, 3031–3040, November 1998

A Polymer Model for the Structural Organization of Chromatin Loops and Minibands in Interphase Chromosomes

Joseph Ostashevsky

Department of Radiation Oncology, State University of New York, Health Science Center at Brooklyn, Brooklyn, New York 11203

Submitted May 15, 1998; Accepted August 21 1998
Monitoring Editor: Joseph Gall

A quantitative model of interphase chromosome higher-order structure is presented based on the isochore model of the genome and results obtained in the field of copolymer research. G1 chromosomes are approximated in the model as multiblock copolymers of the 30-nm chromatin fiber, which alternately contain two types of 0.5- to 1-Mbp blocks (R and G minibands) differing in GC content and DNA-bound proteins. A G1 chromosome forms a single-chain string of loop clusters (micelles), with each loop ~1–2 Mbp in size. The number of ~20 loops per micelle was estimated from the dependence of geometrical versus genomic distances between two points on a G1 chromosome. The greater degree of chromatin extension in R versus G minibands and a difference in the replication time for these minibands (early S phase for R versus late S phase for G) are explained in this model as a result of the location of R minibands at micelle cores and G minibands at loop apices. The estimated number of micelles per nucleus is close to the observed number of replication clusters at the onset of S phase. A relationship between chromosomal and nuclear sizes for several types of higher eukaryotic cells (insects, plants, and mammals) is well described through the micelle structure of interphase chromosomes. For yeast cells, this relationship is described by a linear coil configuration of chromosomes.

INTRODUCTION

The higher-order structure of interphase chromosomes is still poorly understood. Many models in the literature include a loop structure as one of the high levels of packing of a chromatin fiber in the nucleus (for review see van Holde, 1989; Wolffe, 1995). Earlier studies have suggested that an average chromatin loop contains ~50–100 kbp DNA (van Holde, 1989; Wolffe, 1995), whereas more recent studies suggest large loops of ~1–3 Mbp, which may include 50- to 100-kbp loops (Razin and Gromova, 1995; Sachs *et al.*, 1995; Yokota *et al.*, 1995; Johnston *et al.*, 1997).

On the scale of 1–3 Mbp, high-resolution mapping of replication bands in S phase (Drouin *et al.*, 1990, 1994) is similar to a quasiperiodic pattern of G (for dark in Giemsa) and R (for reverse, light in Giemsa) minibands observed in prophase chromosomes (Bak *et al.*, 1981; Yunis, 1981). G minibands are AT rich, late replicating, and gene poor, whereas R minibands are GC and gene rich and early replicating and contain a less compact chromatin than do G minibands (Holmquist, 1992; Craig and Bickmore, 1993; Yokota *et al.*, 1997). Isochores, long DNA segments having a size range from 0.2 to 1.3 Mbp with an excess of one type of nucleotide (e.g., AT rich or GC rich), are found in the genome of higher eukaryotes (Bernardi, 1995).

An important feature of G1 phase chromosomes is that they behave approximately as ideal Gaussian chains, which obey random-walk statistics (van den Engh *et al.*, 1992; Sachs *et al.*, 1995; Yokota *et al.*, 1995). This was concluded from the proportionality between the mean square geometrical distance between two points on the chromosome and their genomic distance, on the scale up to ~1 Mbp. On a larger scale (up to 200 Mbp), this dependence has a much shallower slope

Author's E-mail address: ostasj23@hscbklyn.edu.

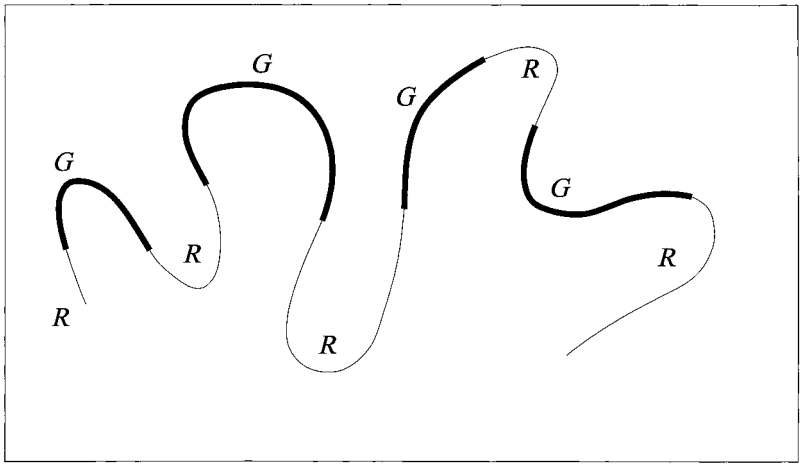

Figure 1. A mammalian G1 chromosome is approximated as a multiblock copolymer containing two types of polymer blocks with different GC contents. Light and dark chromatin segments are R and G blocks, respectively.

than the initial one (Sachs *et al.*, 1995; Yokota *et al.*, 1995).

On the nuclear level, G1 chromosomes tend to occupy exclusive territories rather than overlapping extensively (Haaf and Schmid, 1991; Cremer *et al.*, 1993; Zirbel *et al.*, 1993; van Driel *et al.*, 1995; Kurz *et al.*, 1996; Ferreira *et al.*, 1997; Zink *et al.*, 1998). There is some contradiction between the random-walk behavior of chromatin and the discreteness of chromosomal domains: random coils do not have clear boundaries, and they are prone to overlap (de Gennes 1979; Grosberg and Khokhlov, 1994).

The size of a nucleus influences the compactness of individual chromosomes (Yokota *et al.*, 1995, 1997; Sanchez *et al.*, 1997). Compartmentalization of nuclear space is characteristic for chromosome functions (Spector, 1993; Strouboulis and Wolffe, 1996). In particular, DNA replication starts only in several hundred clusters per nucleus in early S phase (for review see Berezney *et al.*, 1995a; Jackson and Cook, 1995).

Several polymer approaches to chromosomes exist in the literature (van den Engh *et al.*, 1992; Hahnfeldt *et al.*, 1993; Ostashevsky and Lange, 1994; Sikorav and Jannink, 1994; Duplantier *et al.*, 1995; Sachs *et al.*, 1995; Jannink *et al.*, 1996; Ostashevsky, 1996, 1998; Houchmandzadeh *et al.*, 1997; Liu and Sachs, 1997; Marko and Siggia, 1997a); however, only a few articles consider interphase chromosomes.

This study develops a model of the higher-order structure of interphase chromosomes that deals with the problems and takes into account the main facts mentioned above. In this model, based on the isochore model of the genome (Bernardi, 1995) and results obtained in the field of copolymer research (e.g., see Semenov *et al.*, 1995, 1996), a G1 chromosome is approximated as a multiblock copolymer containing two types of blocks differing in GC content.

RESULTS AND DISCUSSION

The Model's Background

The presented model of interphase chromosomes is based on the following assumptions.

1) A mammalian G1 chromosome can be approximated as a multiblock copolymer alternately containing two types of polymer blocks different in GC content (Figure 1). This assumption is supported by the observation that the DNA sequence of high eukaryotes is not random but is a mosaic of isochores, which are long DNA segments (0.2–1.3 Mbp) with an excess of one type of nucleotides (AT or GC) (Bernardi, 1995). Although five families of isochores can be defined in mammalian genomes, the division of polymer blocks in two classes, R (GC rich) and G (AT rich), as made in the presented model, can be considered as a first approximation. It is argued below that the R and G blocks in the model are related to the interphase and prophase R and G minibands, which are ~1 Mbp in size (Bak *et al.*, 1981; Yunis, 1981; Ronne *et al.*, 1995); thus, the terms blocks and minibands will be used interchangeably in this article.

2) A multiblock copolymer containing two alternately located types of blocks can form a single-chain string of loop clusters called micelles (Halperin, 1991). A micelle consists of a certain number of loops, the termini of which, formed by blocks of one type, are located in close proximity to each other (Figure 2). Micelle structures are well studied for diblock copolymers (polymer chains having only two blocks) and ionomers (polymer chains with charged groups at the ends) (e.g., see Semenov *et al.*, 1995, 1996). Large multiblock copolymers form single-chain micelles, and small diblock copolymers form multichain micelles. Formation of loops and organization of them in micelles constitute an entropically unfavorable process, because the number of possible polymer confor-

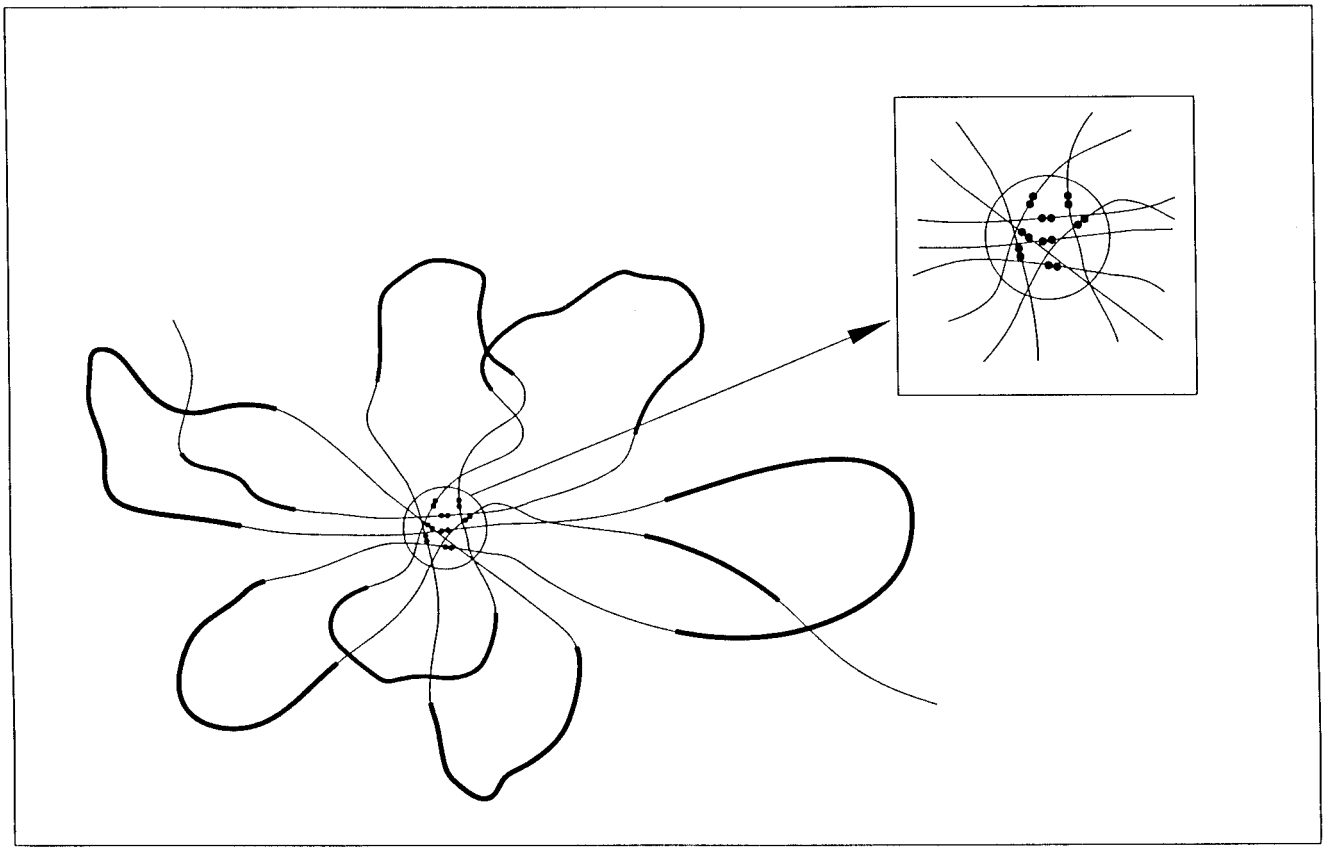

Figure 2. Schematic drawing of a micelle in a G1 chromosome. Dark and light chromatin blocks are G and R minibands, respectively. Segments drawn with free ends can be either chromosome ends or intermicelle links. The circle represents the micelle core (see inset), where loop termini are located. The dark dots at loop termini represent multiprotein complexes, e.g., replication complexes.

mations decreases, but it occurs in multiblock copolymers because of the energically favorable processes of repulsion between unlike monomer units and/or attraction between like monomer units (de Gennes 1979; Grosberg and Khokhlov, 1994). For a multiblock copolymer in aqueous solution, which contains two types of blocks with hydrophobic and hydrophilic groups, hydrophobic blocks form loop termini at the micelle cores, and hydrophilic blocks are located at loop apices.

3) Incompatibility between GC- and AT-rich blocks can contribute to micelle formation. On average, R minibands are at least ~3% richer in GC content than G minibands (Saitoh and Laemmli, 1994). Approximately 80% of the known genes are found in R minibands (Craig and Bickmore, 1993). This suggests that more histones are chemically modified, e.g., acetylated, in R than in G blocks, and more transcription complexes are bound to R than to G blocks. Because of the large size of the blocks (0.5–1 Mbp), even a small difference in interaction energy per monomer between unlike versus like monomers can lead to block separation: the blocks of one type form the loop termini, and the blocks of the other type are located at loop apices. Marko and Siggia (1997a) suggested that one can determine the parameters of the GC versus AT incompatibility by mixing bacterial DNA molecules that have very different GC contents.

Another contribution to stabilization of the chromosome micelle structure could come from multiprotein complexes, which participate in many chromosome functions at various stages of the cell cycle, e.g., transcription, replication, and chromosome condensation. Multiprotein complexes may associate differently with R and G blocks, as was suggested above for transcription complexes. For DNA replication, we assume that replication complexes are located in the micelle cores at the onset of S phase (see below).

4) The average loop size in interphase chromosomes in the model is assumed to be in the range of 1–2 Mbp. This is consistent with a loop containing two isochores or two replication minibands of size 0.5–1.0 Mbp, which seems to be reasonable (Bernardi, 1995; Simon and Cedar, 1996). The range of loop sizes for a large number of mammalian cell lines was estimated to be between 1.2 and 2.2 Mbp (Johnston *et al.*, 1997). In the

nuclei of early embryos of *Drosophila*, contacts between chromatin and the nuclear envelope have a frequency of one per 1–2 Mbp (Marshall *et al.*, 1996). Because a loop contacts the nuclear envelope at its apex in the presented model, this leads to a 1- to 2-Mbp loop size.

Some Properties of Chromatin and Micelles

Individual loops in micelles behave as independent Gaussian coils. On the other hand, micelles are not interpenetrating (Semenov *et al.*, 1995). Thus, the micelle structure of interphase chromosomes reconciles the contradiction mentioned in the INTRODUCTION between the discreetness of chromosomal territories and the random-walk behavior of chromatin.

Random-walk behavior of chromatin was demonstrated (van den Engh *et al.*, 1992; Sachs *et al.*, 1995; Yokota *et al.*, 1995, 1997) by the linear dependence of the mean square of the geometrical distance between two probes on the same chromosome, $\langle h_x^2 \rangle$ (μm^2), versus their genomic distance, M_x (Mbp):

$$\langle h_x^2 \rangle = BM_x \quad (1)$$

where the coefficient B (μm^2/Mbp) describes chromatin compactness. Equation *1* is valid on the scale up to ~1 Mbp, no matter where two probes are located on the chromosome, and deviations from the linear dependence are observed for $M_x > 1$ Mbp. Equation *1* describes the behavior of ideal Gaussian chains, which particularly occurs in polymer melts or θ solvents (de Gennes 1979; Grosberg and Khokhlov, 1994). Although the conditions for chromosomes in nuclei might not be the same as in a melt or a θ solvent, here we consider ideal Gaussian chains as a first approximation, because the values of B have been obtained using this assumption (van den Engh *et al.*, 1992; Sachs *et al.*, 1995; Yokota *et al.*, 1995, 1997).

It is known (e.g., see de Gennes, 1979) that $\langle h_x^2 \rangle$ can also be represented as $\langle h_x^2 \rangle = bL_x$, where b is the length of the Kuhn statistical segment, and L_x is the fiber contour length. These two quantities are interrelated through k, the mass of the Kuhn statistical segment, and M_x: $b/k = L_x/M_x$. Thus, B in Eq. *1* can be expressed as $B = b^2/k$.

Because the 30-nm chromatin fiber has ~0.2 kbp per nucleosome (van Holde, 1989; Wolffe, 1995), n, the number of nucleosomes per 10 nm of chromatin fiber contour length, can be estimated from the above expressions, as:

$$n = A(b/B) \quad (2)$$

where the coefficient A = 50 μm/Mbp (=10 nm/0.2 kbp).

It has been shown that values of B for chromatin in R minibands are ~2.5-fold greater than those in G minibands, independent of fixation technique (Yokota *et al.*, 1997). The fixation technique strongly affects the absolute values of B_G and B_R (values of B for G and R minibands, respectively), in parallel with nuclear size (Sachs *et al.*, 1995; Yokota *et al.*, 1995, 1997). For paraformaldehyde-fixed human fibroblast nuclei, nuclear size is not changed by fixation, and $B_G = 0.5$ μm^2/Mbp and $B_R = 1.3$ μm^2/Mbp (Yokota *et al.*, 1997). We shall use these values and their average value B = 0.9 μm^2/Mbp for the calculations below.

The larger value of B_R relative to B_G means that chromatin in R minibands is stretched in comparison with that in G minibands. In the accordion-like structure of the chromatin fiber (Woodcock *et al.*, 1993; Horowitz *et al.*, 1994; Woodcock and Horowitz, 1995), angles between links increase under stretching, which leads to an increase in the ratio of chromatin contour length to chromatin mass, L/M, which = b/k, and an increase in b/k leads to an increase in the values of B (see above).

Experimental data (Castro 1994; also see Marko and Siggia, 1997b) indicate that the Kuhn segment length b ~ 60 nm. Substituting $B_G = 0.5$ μm^2/Mbp and $B_R = 1.3$ μm^2/Mbp, and b = 60 nm in Eq. *2*, one obtains n = 6 and 2.3 nucleosomes per 10-nm contour length for G and R minibands, respectively. These values are consistent with experimental data for chromatin structure: n = 6–8 nucleosomes per 10 nm for a compact chromatin fiber and n = 1–2 nucleosomes per 10 nm for a stretched chromatin fiber (van Holde and Zlatanova, 1995, 1996; Woodcock and Horowitz, 1995).

It has been shown for micelles that the polymer blocks that form micelle cores are stretched (see e.g., Semenov *et al.*, 1995, 1996), because a large block incompatibility favors an increase in micelle size, and this leads to stretching of polymer blocks in the micelle cores. Applied to R and G minibands in chromatin micelles, this suggests that R blocks, which are stretched, are located at loop termini, and G blocks, which are unstretched, are located at loop apices. This assignment of R and G minibands is consistent with their replication time patterns (see below).

Dependence of Mean-Square Geometrical Distance on Genomic Distance for G1 Phase Chromosomes

The dependence of mean-square geometrical distance, $\langle h_x^2 \rangle$, on genomic distance, M_x, has been obtained on the 0.1–200 Mbp scale for three chromosomes (4, 5, and 19) in fixed human fibroblasts (Sachs *et al.*, 1995; Yokota *et al.*, 1995). These data can be summarized as having experimental points located between two parallel lines that have a shallow slope of ~20-fold less than the slope of this dependence over a short range (<1 Mbp). The authors suggested a model of chromosome structure that includes ~3-Mbp loops containing flexible chromatin that corresponds to a steep slope and a much less flexible nonchromatin backbone that

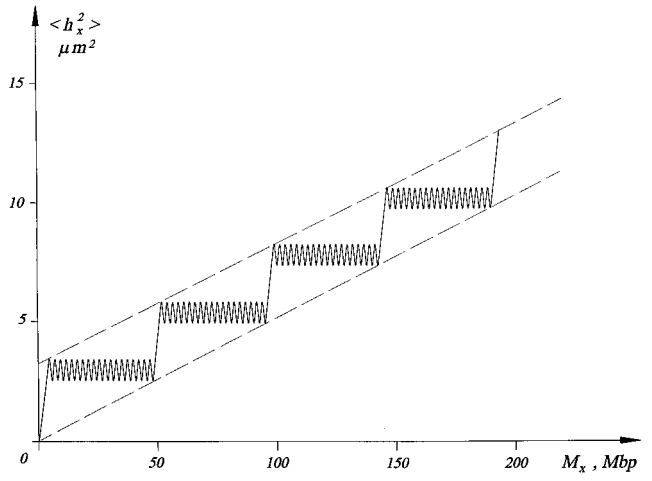

Figure 3. Schematic drawing of the dependence of $\langle h_x^2 \rangle$, mean-square geometrical distance, vs. M_x, genomic distance between two points on a G1 chromosome. The $\langle h_x^2 \rangle$ vs. M_x dependence is due to chromosome tails and intermicelle links, because the net increase in $\langle h_x^2 \rangle$ inside a micelle is zero. Dashed lines represent the boundaries of the experimental points. The model predicts that their slope (B_{app}) is f-fold shallower than the initial slope (see Eq. *6*), where f is the average number of loops per micelle.

corresponds to a shallow slope (also see Liu and Sachs, 1997). However, the measurements under separation of <1 Mbp, wherever one looks in the chromosome, never reveal a shallow slope (Yokota *et al.* 1995, 1997); this puts in doubt the existence of a rigid backbone.

The presented model suggests that intermicelle links and micelle tails contain the same material as micelle loops, the 30-nm chromatin fiber. The $\langle h_x^2 \rangle$ versus M_x dependence following from this model is presented schematically in Figure 3. The net increase in $\langle h_x^2 \rangle$ inside a micelle is zero, because the loop termini are located randomly and very close to each other in the micelle core. Thus, the $\langle h_x^2 \rangle$ versus M_x dependence in the model is due to chromosome tails and intermicelle links.

Let us consider the $\langle h_x^2 \rangle$ versus M_x dependence quantitatively. Suppose a G1 chromosome of size M_o (megabase pairs) forms several micelles with an average loop size, M_f (megabase pairs), and an average number of loops per micelle, f. The number of micelles per chromosome, m, can be expressed as:

$$m \approx M_o/fM_f \tag{3}$$

As shown in Figure 3, straight lines for the boundaries of the experimental points can be defined as those connecting a telomere and the opposite tail base. Both lines have the same slope, B_{app}, which can be defined as:

$$\langle H^2 \rangle = B_{app}(M_o - M_f) \approx B_{app}M_o \tag{4}$$

On the other hand, the same mean-square distance can be expressed as caused by a chromosome tail and the m-1 intermicelle links:

$$\langle H^2 \rangle = mBM_f = BM_o/f \tag{5}$$

Equating Eqs. *4* and *5*, one obtains the expression for the average number of loops per micelle, f:

$$f = B/B_{app} \tag{6}$$

The meaning of Eq. *6* is that because there is one linear intermicelle link per f loop, representation of micelle structure as a linear coil yields a slope = B_{app}, which is f-fold shallower than that for the micelle. The estimate of f from Eq. *6* is independent of any parameter of the model and equals the ratio of two measurable values, which was found to be ~20 (Sachs *et al.*, 1995; Yokota *et al.*, 1995). Thus, data for the geometrical versus genomic distances for human G1 fibroblasts (Sachs *et al.*, 1995; Yokota *et al.*, 1995) suggest that the average number of loops per micelle, f, is ~20 in these cells.

The number of loops per micelle in G1 fibroblast chromosomes (f ~ 20) is comparable with the number of loops per micelle for ionomers, which is 5–50 (Semenov *et al.*, 1995, 1996). The value of f is limited by the maximal number of polymer chains that can be brought together in a micelle core (Semenov *et al.*, 1996).

A crude estimate of f_{lim}, the maximal number of loops per micelle, is as follows. The number of loop termini confined in the micelle core is ≈f, the number of loops per micelle (exactly f + 1). Suppose D_c is the micelle core diameter, L is the loop terminus contour length, and h is the distance between the entrance and exit points of a loop terminus. The total volume occupied by chromatin fibers in the micelle core is $\approx fd^2L$, where d is the chromatin fiber diameter (=30 nm). The average contour length, L, can be expressed as $\langle h^2 \rangle/b$ (see above), where $\langle h^2 \rangle$, the mean-square average cord length in a sphere, = $D_c^2/2$, and b is the Kuhn segment length (=60 nm). Equating the total volume occupied by loop termini to the micelle core volume = $\pi D_c^3/6$, one can estimate f_{lim} as:

$$f_{lim} \approx (\pi/3)bD_c/d^2 \tag{7}$$

It is argued below that chromatin replication starts at the micelle cores. Taking the diameter of replication "factories" (~0.2–0.3 μm [Hozak *et al.*, 1993; Tomilin *et al.*, 1995]) as a range of D_c, Eq. *7* yields f_{lim} ~ 10–20; this is comparable with the value of f estimated above.

The number of micelles per G1 nucleus, N_m, can be estimated as:

$$N_m = C/fM_f \tag{8}$$

where C is the G1 DNA content. Diploid human cells have C = 6.4 Gbp, and for f = 20 and M_f = 1–2 Mbp, Eq. *8* yields N_m = 160–320. This estimate is important for discussion of the relationship between micelle structure and DNA replication.

Micelle Structure and DNA Replication

In high eukaryotes, but not in yeast, chromosome structure plays an important role in replication initiation (Coverley and Laskey, 1994; Laskey and Madine, 1996; Gilbert, 1998). Let us show that the proposed model is consistent with data for early S phase replication in mammalian cells if we suggest that at the onset of S phase, chromatin replication is initiated at the loop termini in micelle cores. The following points support this suggestion.

1) If replication starts in the micelle cores, R blocks that form loop termini (see above) should replicate earlier than G blocks. This is consistent with the fact that R minibands replicate earlier than G minibands (for review see Drouin *et al.*, 1994). Thus, in this model two features of R minibands, stretched chromatin and early replication, could be explained by their location in micelle cores.

2) In the model, chromatin fibers contact the nuclear membrane at loop apices. Thus, the observation that the nuclear periphery contains predominantly late-replicated G minibands (Ferreira *et al.*, 1997) is consistent with the assignment of G minibands to loop apices.

3) If replication starts in the micelle cores at the beginning of S phase: a) the number of replication clusters per nucleus should be similar to the number of micelle cores (N_m) in G1 phase; b) the number of minifoci per cluster should be similar to the number of loop termini per core (f); and thus, c) the total number of minifoci per nucleus should be similar to the product fN_m. At the onset of S phase, nuclei with C ~ 6 Gbp (e.g., diploid human fibroblasts and V79 cells) have 100–300 replication clusters with ~20 minifoci per cluster (Berezney *et al.*, 1995a; Jackson and Cook, 1995); this is consistent with the estimates obtained above: N_m = 160–320 and f ~ 20. Cell lines with C = 9–10 Gbp (e.g., mouse 3T3 and human HeLa) have 600–750 replication clusters with ~10–12 minifoci per cluster (Jackson and Pombo, 1998), or a total number ~6000–9000 minifoci per nucleus, which is consistent with $fN_m = C/M_f$ = 4500–10000 for these cells. These data suggest that f is ~10–20 for various cells.

4) Replication-labeled clusters were observed through several cell cycles (Jackson and Pombo, 1998), and their number doubles in G2 versus G1 (Jackson and Pombo, 1998; Zink *et al.*, 1998). The size of these labeled chromatid subdomains is ~0.4–0.8 μm (Zink *et al.*, 1998). This is comparable with our estimate of the size range of G and R minibands, i.e., 0.5–1.1 μm (=$[BM_f/2]^{1/2}$, see Eq. *1*) for B = 0.5–1.3 μm^2/Mbp (Yokota *et al.*, 1997) and M_f = 1–2 Mbp.

Thus, the suggestion that replication clusters can be considered a fundamental aspect of the higher-order structure of the genome (Berezney *et al.*, 1995b; Jackson and Pombo, 1998; Zink *et al.*, 1998) can have micelle cores as its basis.

Relationship Between Size of Interphase Nucleus and Chromosome Compactness

One test of the model is that the chromosome size estimated with the model must not exceed the size (length and thickness) of the corresponding nucleus, and that the total chromosomal volume or area must not exceed the nuclear volume or area. To estimate the micelle diameter, a micelle can be represented as a star-branched polymer with branch size of $M_f/2$. Because chromatin in loops behaves as a Gaussian chain, and because the branch ends are close to each other in the micelle core, the mean-square micelle diameter, $\langle D_m^2 \rangle$, is equal to double the mean-square branch size:

$$\langle D_m^2 \rangle = BM_f \tag{9}$$

where the average value $B = (B_G + B_R)/2$.

For human fibroblasts, replacing M_f = 1–2 Mbp and B = 0.9 μm^2/Mbp in Eq. *9*, one obtains $\langle D_m^2 \rangle^{1/2}$ = 0.9–1.3 μm, which is close to the smallest nuclear thickness measured for cultured cells (=1.2 μm) observed for human AG1522 fibroblasts in monolayer (Raju *et al.*, 1991). This suggests a two-dimensional (2-D) organization of micelles in a monolayer of flattened AG1522 cells.

The mean-square chromosome length, $\langle H^2 \rangle$, can be presented as the end-to-end distance for a random walk of m micelles, each of length (diameter) D_m. Replacing D_m and m from Eqs. *3* and *9*, one obtains:

$$\langle H^2 \rangle = D_m^2 m = BM_o/f \tag{10}$$

Equation *10* is the same as Eq. *5*, where the expression for $\langle H^2 \rangle$ was obtained as a random walk of the inter-micelle links. Thus, two approaches yield the same values of H. For human fibroblasts, replacing f = 20 and B = 0.9 μm^2/Mbp in Eq. *10*, one obtains $\langle H^2 \rangle^{1/2}$ ~ 4 μm for the largest (M_o = 263 Mbp) human chromosome. For a fibroblast in monolayer, this is much smaller than its nuclear dimensions (~10–30 μm [Yokota *et al.*, 1997]).

The 2-D chromosome territories have been measured for chromosomes 17 (=4.1 μm^2; M_o = 92 Mbp) and the inactive X (=5.2 μm^2; M_o = 164 Mbp), respectively, in human fibroblasts (Clemson *et al.*, 1996). For a chromosome consisting of m micelles, the 2-D chromosome area, A_c, can be presented as a sum of micelle areas, = $(\pi/4)D_m^2 m$, which is only slightly different from the expression for $\langle H^2 \rangle$ (see Eq. *10*). It follows

Table 1. Relationship between nuclear volume and coefficient *B*

Cells	*C* (Gbp)	V_n (μm^3)	C/V_n (Mbp/μm^3)	*B*[a] (μm^2/Mbp)	*n*[b] nucleosomes (per 10 nm)
Series of 30 plants (Baetcke *et al.*, 1967)			62	0.2–0.5	6–13
Lymphocyte	6.4	110[c]	58	0.2–0.5	6–12
AG1522	6.4	220[d]	29	0.4–0.8	4–8
Series of 18 mammalian cell lines (Sontag *et al.*, 1990)			24	0.4–0.9	3–7
Drosophila	0.33	30[e]	11	0.7–1.5	2–4
S. cerevisiae	0.025	11[f]	2.2	0.6[g]	5

[a] Calculated from Eq. *13* for f = 10–20, M_f = 1–2 Mbp, and $\alpha = \pi/6$.

[b] Calculated from Eq. *2* for b = 60 nm.

[c] Volume of sphere of 6 μm diameter.

[d] Calculated from $V_n = (4/\pi)SH$, where S and H, the mean nuclear area and thickness, respectively, are taken from Table 1 in Raju *et al.*, 1991.

[e] Calculated from volumes of polytene nucleus (Hochstrasser and Sedat, 1987) under the assumption that the nuclear volume doubles after each replication cycle.

[f] Calculated for an average nuclear diameter = 2.8 μm (Guacci *et al.*, 1994).

[g] Calculated from Eq. *14* for a linear coil configuration of chromosomes.

from Eqs. *3* and *9* that $A_c = (\pi/4)BM_o/f$. Thus, B can be estimated from A_c as:

$$B = (4/\pi)A_c f/M_o \quad (11)$$

For f = 20 and the above values of A_c, Eq. *11* yields B = 1.1 and 0.8 μm^2/Mbp for chromosomes 17 and X, respectively. These values are close to the average value of B = 0.9 μm^2/Mbp (Yokota *et al.*, 1997).

Chromosome compactness seems to be adjusted to nuclear size (Yokota *et al.*, 1995, 1997; Sanchez *et al.*, 1997). We shall estimate B from nuclear cross-section areas and nuclear volumes. The test is whether the estimated values of B fall within the range of experimental values. We assume that the chromosomes fill all available space in the nucleus. This assumption is consistent with observations of constrained diffusional motion of chromosomes in the nucleus (Abney *et al.*, 1997; Marshall *et al.*, 1997).

For 2-D nuclei, the available nuclear area is αA_n, where α is the occupancy factor, and A_n is the nuclear cross-section area. Because there is a large number (hundreds) of micelles in a nucleus (see above), the occupancy factor α for tightly packed micelles in a nucleus can be taken to be $\alpha \sim \pi/4$, as for squared circles. Equating the available nuclear area to the sum of micelle areas, $= N_m \pi D_m^2/4$, and using Eqs. *8* and *9*, one obtains an estimate for B from A_n:

$$B = A_n f/C \quad (12)$$

Human HSF7 fibroblasts (C ~ 6 Gbp) and HeLa cells (C ~ 9 Gbp) form a monolayer of flattened cells, and their nuclei may be approximated as 2-D. Experimental values of their nuclear cross-section areas are A_n = 160, 240, and 400 μm^2 for the paraformaldehyde-fixed HSF7 and MAA-fixed HeLa and HSF7 cells, respectively (Yokota *et al.*, 1997). For f = 20, Eq. *12* yields B = 0.5–1.3 μm^2/Mbp, which is close to the experimental values (Yokota *et al.*, 1997).

For 3-D nuclei, the available nuclear volume is αV_n, where V_n is the nuclear volume and α is the occupancy factor, which can be taken to be $\sim\pi/6$, as for cubed spheres. Equating the available nuclear volume to the sum of micelle volumes, $N_m \pi \langle D_m^2 \rangle^{3/2}/6$, and using Eqs. *8* and *9*, one obtains:

$$B = (6\alpha/\pi)^{2/3}(V_n/C)^{2/3}\,(f^{2/3}/M_f^{1/3}) \quad (13)$$

Table 1 presents estimates of B from Eq. *13* for f = 10–20, M_f = 1–2 Mbp, and $\alpha = \pi/6$. It follows from Table 1 that the whole range of estimated B, 0.2–1.5 μm^2/Mbp, is consistent with the range of experimentally determined values (Yokota *et al.*, 1997). The values of n, the number of nucleosomes per 10 nm of chromatin fiber contour length estimated from Eq. *2*, range between 2 and 13, which seems to be reasonable (van Holde and Zlatanova, 1995, 1996; Woodcock *et al.*, 1995).

Equation *13* is not applicable to cells with very small chromosomes, such as the budding yeast *Saccharomyces cerevisiae*, because all or most of their chromosomes are smaller than M_f = 1–2 Mbp. We suggest that yeast chromosomes have a linear coil configuration. Because replication initiation in higher eukaryotes is suggested to begin in the micelle cores (see above), the lack of micelle structure in yeast chromosomes is consistent with the observation that higher and lower eukaryotes have different patterns of replication initiation (see review in Gilbert, 1998).

The expression for B for linear coil polymers (e.g., yeast chromosomes) can be obtained from Eq. *13* by replacing f with 1 and M_f with the average chromosome size $M_o = C/N$, where N is the number of chromosomes per nucleus (N = 32 for *S. cerevisiae*):

$$B = (6\alpha/\pi)^{2/3}(V_n/C)^{2/3}\,(N/C)^{1/3} \qquad (14)$$

Equation *14* yields B = 0.6 μm^2/Mbp for *S. cerevisiae*, which is close to the estimated values of B obtained for the micelle structure of high eukaryote chromosomes (see Table 1). This is consistent with the observation that chromatin in interphase yeast cells has the same relationship between geometrical versus genomic distances as that in mammalian cells on the 1-Mbp scale (Guacci *et al.*, 1994).

CONCLUSIONS

1) A G1 phase mammalian chromosome can be approximated as a multiblock copolymer containing two alternating types (R and G) of polymer blocks, which form a string of loop clusters (micelles), with each loop ~1–2 Mbp in size. Application of the model to the experimental data (Sachs *et al.*, 1995; Yokota *et al.*, 1995) for the dependence of geometrical versus genomic distances between two points on the same chromosome yields an estimate of ~20 loops per micelle.

2) The number of micelles per nucleus is close to the observed number of replication clusters at the onset of S phase, and the number of loops per micelle is close to the number of replication minisites per cluster. This is consistent with loop termini being sites of initiation of DNA replication at the onset of S phase.

3) R minibands form loop termini, whereas G minibands are located at loop apices. This conclusion follows from relating the chromatin fiber being stretched in R minibands (Yokota *et al.*, 1997) to a known feature of micelles, that polymer blocks located in micelle cores are stretched. These locations of R and G minibands are consistent with their replication pattern; the former are replicated earlier than the latter.

4) The chromosome micelle structure describes the relationship between chromosomal and nuclear sizes for several types of higher-order eukaryotic cells (insects, plants, and mammals). For yeast cells, this relationship is described by a linear coil configuration of chromosomes.

ACKNOWLEDGMENTS

I am grateful to C.S. Lange for very helpful discussions and careful reading of the manuscript, A. Berens for drawing the figures, and the anonymous reviewers for their constructive suggestions.

REFERENCES

Abney, J.R., Cutler, B., Fillbach, M.L., Axelrod, D., and Scalettar, B.A. (1997). Chromatin dynamics in interphase nuclei and its implications for nuclear structure. J. Cell Biol. *137*, 1459–1468.

Baetcke, K.P., Sparrow, A.H., Nauman, C.H., and Schwemmer, S.S. (1967). The relationship of DNA content to nuclear and chromosome volumes and to radiosensitivity (LD_{50}). Proc. Natl. Acad. Sci. USA *58*, 533–540.

Bak, A.L., Jorgensen, A.L., and Zeuthen, J. (1981). Chromosome banding and compaction. Hum. Genet. *57*, 199–202.

Berezney, R., Mortillaro, M., Ma, H., Wei, X., and Samarabandu, J. (1995a). The nuclear matrix: a structural millieu for genomic function. Int. Rev. Cytol. *162A*, 1–65.

Berezney, R., Ma, H., Meng, C., Samarabandu, J., and Cheng, P.C. (1995b). Connecting genomic architecture and DNA replication in three dimensions. Zool. Stud. *1*(suppl), 29–32.

Bernardi, G. (1995). The human genome: organization and evolutionary history. Annu. Rev. Genet. *29*, 445–476.

Castro, C.A. (1994). Mechanisms of the Elasticity of Single Chromatin Fibers: The Effect of Histone H1. Ph.D. Thesis. University of Oregon.

Clemson, C.M., McNeil, J.A., Willard, H.F., and Lawrence, J.B. (1996). XIST RNA paints the inactive X chromosome at interphase: evidence for a novel RNA involved in nuclear/chromosome structure. J. Cell Biol. *132*, 259–275.

Coverley, D., and Laskey, R.A. (1994). Regulation of eukaryotic DNA replication. Annu. Rev. Biochem. *63*, 777–792.

Craig, J.M., and Bickmore, W.A. (1993). Chromosome bands—flavours to savour. Bioessays *15*, 349–354.

Cremer, T., *et al*. (1993). Role of chromosome territories in the functional compartmentalization of the cell nucleus. Cold Spring Harbor Symp. Quant. Biol. *58*, 777–792.

de Gennes, P.-G. (1979). Scaling Concepts in Polymer Physics. Ithaca, NY: Cornell University Press.

Drouin, R., Holmquist, G.P., and Richer, C.L. (1994). High-resolution replication bands compared with morphological G- and R-bands. Adv. Hum. Genet. *22*, 47–115.

Drouin, R., Lemieux, N., and Richer, C.L. (1990). Analysis of DNA replication during S phase by means of dynamic chromosome banding at high resolution. Chromosoma *99*, 273–280.

Duplantier, B., Jannink, G., and Sikorav, J.-L. (1995). Anaphase chromatid motion: involvement of type II DNA topoisomerases. Biophys. J. *69*, 1596–1605.

Ferreira, J., Paolella, G., Ramos, C., and Lamond, A.I. (1997). Spatial organization of large-scale chromatin domains in the nucleus: a magnified view of single chromosome territories. J. Cell Biol. *139*, 1597–1610.

Gilbert, D.M. (1998). Replication origins in yeast versus metazoa: separation of the haves and the haves not. Curr. Opin. Genet. Dev. *8*, 194–199.

Grosberg, A.Y., and Khokhlov, A.R. (1994). Statistical Physics of Macromolecules. New York: AIP Press.

Guacci, V., Hogan, E., and Koshland, D. (1994). Chromosome condensation and sister chromatid pairing in budding yeast. J. Cell Biol. *125*, 517–530.

Haaf, T., and Schmid, M. (1991). Chromosome topology in mammalian interphase nuclei. Exp. Cell Res. *192*, 325–332.

Hahnfeldt, P., Hearst, J.E., Brenner, D.J., Sachs, R.K., and Hlatky, L.R. (1993). Polymer models for interphase chromosomes. Proc. Natl. Acad. Sci. USA *90*, 7854–7858.

Halperin, A. (1991). On the collapse of multiblock copolymers. Macromol. *24*, 1418–1419.

Hochstrasser, M., and Sedat, J.W. (1987). Three-dimensional organization of *Drosophila melanogaster* interphase nuclei. I. Tissue-specific aspects of polytene nuclear architecture. J. Cell Biol. *104*, 1455–1470.

Holmquist, G.P. (1992). Chromosome bands, their chromatin flavors, and their functional features. Am. J. Hum. Genet. *51*, 17–37.

Horowitz, R.A., Agard, D.A., Sedat, J.W., and Woodcock, C.L. (1994). The three-dimensional architecture of chromatin in situ: electron tomography reveals fibers composed of a continuously variable zig-zag nucleosome ribbon. J. Cell Biol. *125*, 1–10.

Houchmandzadeh, B., Marko, J.F., Chatenay, D., and Libchaber, A. (1997). Elasticity and structure of eukaryote chromosomes studied by micromanipulation and micropipette aspiration. J. Cell Biol. *139*, 1–12.

Hozak, P., Hassan, A.B., Jackson, D.A., and Cook, P.R. (1993). Visualization of replication factories attached to a nucleoskeleton. Cell *73*, 361–373.

Jackson, D.A., and Cook, P.R. (1995). The structural basis of nuclear function. Int. Rev. Cytol. *162A*, 125–149.

Jackson, D.A., and Pombo, A. (1998). Replicon clusters are stable units of chromosome structure: evidence that nuclear organization contributes to the efficient activation and propagation of S phase in human cells. J. Cell Biol. *140*, 1285–1295.

Jannink, G., Duplantier, B., and Sikorav, J.-L. (1996). Forces on chromosomal DNA during anaphase. Biophys. J. *71*, 451–465.

Johnston, P.J., Olive, P.L., and Bryant, P.E. (1997). High-order chromatin structure-dependent repair of DNA double-strand breaks: modeling the elution of DNA from nucleoids. Radiat. Res. *148*, 561–567.

Kurz, A., Lampel, S., Nikolenko, J.E., Bradl, J., Benner, A., Zirbel, R.M., Cremer, T., and Lichter, P. (1996). Active and inactive genes localize preferentially in the periphery of chromosome territories. J. Cell Biol. *135*, 1195–1205.

Laskey, R., and Madine, M. (1996). Role of nuclear structure in DNA replication. In: DNA Replication in Eukaryotic Cells, ed. M.L. DePamphilis, Cold Spring Harbor, NY: Cold Spring Harbor Laboratory Press, 387–408.

Liu, B., and Sachs, R.K. (1997). A two-backbone polymer model for interphase chromosome geometry. Bull. Math. Biol. *59*, 325–337.

Marko, J.F., and Siggia, E.D. (1997a). Polymer models of meiotic and mitotic chromosomes. Mol. Biol. Cell *8*, 2217–2231.

Marko, J.F., and Siggia, E.D. (1997b). Driving proteins off DNA using applied tension. Biophys. J. *73*, 2173–2178.

Marshall, W.F., Dernburg, A.F., Harmon, B., Agard, D.A., and Sedat, J.W. (1996). Specific interactions of chromatin with the nuclear envelope: positional determination within the nucleus in *Drosophila melanogaster*. Mol. Biol. Cell *7*, 825–842.

Marshall, W.F., Straight, A., Marko, J.F., Swerdlow, J., Dernburg, A., Belmont, A., Murray, A.W., Agard, D.A., and Sedat, J.W. (1997). Interphase chromosomes undergo constrained diffusional motion in living cells. Curr. Biol. *7*, 930–939.

Ostashevsky, J.Y. (1996). Centromeric locations in karyotypes: a rule derived from the theory of branched polymers. J. Theor. Biol. *181*, 293–298.

Ostashevsky, J.Y. (1998). Gaussian-chain model for the formation of chromosome aberrations. Radiat. Res. *149*, 179–186.

Ostashevsky, J.Y., and Lange, C.S. (1994). The 30 nm chromatin fiber as a flexible polymer. J. Biomol. Struct. Dyn. *11*, 813–820.

Raju, M.R., Eisen, Y., Carpenter, S., and Inkret, W.C. (1991). Radiobiology of α particles. III. Cell inactivation by α-particle transversals of the cell nucleus. Radiat. Res. *128*, 204–209.

Razin, S.V., and Gromova, I.I. (1995). The channels model of nuclear matrix structure. Bioessays *17*, 443–450.

Ronne, M., Gyldenholm, A.O., and Storm, C.O. (1995). Minibands and chromosome structure: a theory. Anticancer Res. *15*, 249–254.

Sachs, R.K., van den Engh, G., Trask, B.J., Yokota, H., and Hearst, J. (1995). A random-walk/giant-loop model for interphase chromosomes. Proc. Natl. Acad. Sci. USA *92*, 2710–2714.

Saitoh, Y., and Laemmli, U.K. (1994). Metaphase chromosome structure: bands arise from a differential folding path of the highly AT-rich scaffold. Cell *76*, 609–622.

Sanchez, J.A., Karni, R.J., and Wangh, L.J. (1997). Fluorescent in situ hybridization (FISH) analysis of the relationship between chromosome location and nuclear morphology in human neutrophils. Chromosoma *106*, 168–177.

Semenov, A.N., Joanny, J.-F., and Khokhlov, A.R. (1995). Associating polymers: equilibrium and linear viscoelasticity. Macromol. *28*, 1066–1075.

Semenov, A.N., Nyrkova, I.A., and Khokhlov, A.R. (1996). Statistics and dynamic of ionomer systems. In: Ionomers: Characterization, Theory and Applications, ed. S. Schlick, Boca Raton, FL: CRC Press, 251–279.

Sikorav, J.-L., and Jannink, G. (1994). Kinetics of chromosome condensation in the presence of topoisomerases: a phanton chain model. Biophys. J. *66*, 827–837.

Simon, I., and Cedar, H. (1996). Temporal order of DNA replication. In: DNA Replication in Eukaryotic Cells, ed. M.L. DePamphilis, Cold Spring Harbor, NY: Cold Spring Harbor Laboratory Press, 387–408.

Sontag, W., Knedlitschek, G., Weibezahn, K.F., and Dertinger, H. (1990). The DNA content of some mammalian cells measured by flow cytometry and its influence on radiation sensitivity. Int. J. Radiat. Biol. *57*, 1183–1193.

Spector, D. (1993). Macromolecular domains within the cell nucleus. Annu. Rev. Cell Biol. *9*, 265–315.

Strouboulis, J., and Wolffe, A.P. (1996). Functional compartmentalization of the nucleus. J. Cell Sci. *109*, 1991–2000.

Tomilin, K., Solovjeva, L., Krutilina, R., Chamberland, C., Hancock, R., and Vig, B. (1995). Visualization of elementary DNA replication units in human nuclei corresponding in size to DNA loop domains. Chromosome Res. *3*, 32–40.

van den Engh, G., Sachs, R., and Trask, B.J. (1992). Estimating genomic distance from DNA sequence location in cell nuclei by a random walk model. Science *257*, 1410–1412.

van Driel, R., Wansink, D., van Steensel, B., Grande, M.A., Schul, W., and de Jong, L. (1995). Nuclear domains and the nuclear matrix. Int. Rev. Cytol. *162A*, 151–189.

van Holde, K.E. (1989). Chromatin. New York: Springer-Verlag.

van Holde, K.E., and Zlatanova, J. (1995). Chromatin higher order structure: chasing a mirage? J. Biol. Chem. *270*, 8373–8376.

van Holde, K.E., and Zlatanova, J. (1996). What determines the folding of the chromatin fiber? Proc. Natl. Acad. Sci. USA *93*, 10548–10555.

Wolffe, A.P. (1995). Chromatin: Structure and Function, 2nd ed, London: Academic Press.

Woodcock, C.L., Grigoryev, S.A., Horowitz, R.A., and Whitaker, N. (1993). A chromatin folding model that incorporates linker variability generates fiber resembling the native structures. Proc. Natl. Acad. Sci. USA *90*, 9021–9025.

Woodcock, C.L., and Horowitz, R.A. (1995). Chromatin organization re-viewed. Trends Cell Biol. *5*, 272–277.

Yokota, H., Singer, M.J., van den Engh, and Trask, B.J. (1997). Regional differences in the compactness of chromatin in human G_0/G_1 interphase nuclei. Chromosome Res. *5*, 157–166.

Yokota, H., van den Engh, G., Hearst, J.E., Sachs, R.K., and Trask, B.J. (1995). Evidence for the organization of chromatin in megabase pair-size loops arranged along a random-walk path in the human G0/G1 interphase nucleus. J. Cell Biol. *130*, 1239–1249.

Yunis, J.J. (1981). Mid-prophase human chromosomes. The attainment of 2000 bands. Hum. Genet. *56*, 293–298.

Zink, D., Cremer, T., Saffrich, R., Fischer, R., Trendelenburg, M.F., Ansorge, W., and Stelzer, E.H.K. (1998). Structure and dynamics of human interphase chromosome territories in vivo. Hum. Genet. *102*, 241–251.

Zirbel, R.M., Mathieu, U.R., Kurz, A., Cremer, T., and Lichter, P. (1993). Evidence for a nuclear compartment of transcription and splicing located at chromosome domain boundaries. Chromosome Res. *1*, 93–106.